Fish and Shellfish Immunology 81 (2018) 284–296

Contents lists available at ScienceDirect

Fish and Shellfish Immunology

journal homepage: www.elsevier.com/locate/fsi

Full length article

Differentially expressed genes in hemocytes of *Litopenaeus vannamei* challenged with *Vibrio parahaemolyticus* AHPND (VP_{AHPND}) and VP_{AHPND} toxin

Benedict A. Maralit[a,1,2], Phattarunda Jaree[a,1], Pakpoom Boonchuen[a], Anchalee Tassanakajon[a,b], Kunlaya Somboonwiwat[a,b,*]

[a] Center of Excellence for Molecular Biology and Genomics of Shrimp, Department of Biochemistry, Faculty of Science, Chulalongkorn University, Thailand
[b] Omics Science and Bioinformatics Center, Faculty of Science, Chulalongkorn University, Thailand

ARTICLE INFO

Keywords:
Shrimp
Transcriptome
Early mortality syndrome
Hemocyte
Immune system

ABSTRACT

While toxin-harboring *Vibrio parahaemolyticus* has been previously established as the causative agent of early mortality syndrome (EMS) or acute hepatopancreatic necrosis disease (AHPND) in shrimp, information on the mechanistic processes that happen in the host during infection is still lacking. Here, we examined the expression responses of the shrimp hemocyte transcriptome to *V. parahaemolyticus* AHPND (VP_{AHPND}) by RNA sequencing (RNA-seq). Using libraries (SRA accession number SRP137285) prepared from shrimp hemocytes under experimental conditions, a reference library was *de novo* assembled for gene expression analysis of VP_{AHPND}-challenged samples at 0, 3/6, and 48 h post infection (hpi). Using the library from 0-hpi as the control, 359 transcripts were found to be differentially expressed in the 3/6-hpi library, while 429 were differentially expressed in the 48-hpi library. The expression patterns reported in the RNA-seq of 9 representative genes such as anti-lipopolysaccharide factor (*Lv*ALF), crustin p (CRU), serpin 3 (SER), C-type lectin 3 (CTL), clottable protein 2 (CLO), mitogen-activated protein kinase kinase 4 (MKK4), P38 mitogen-activated protein kinase (P38), protein kinase A regulatory subunit 1 (PKA) and DNAJ homolog subfamily C member 1-like (DNJ) were validated by qRT-PCR. The expression of these genes was also analyzed in shrimp that were injected with the partially purified VP_{AHPND} toxin. A VP_{AHPND} toxin-responsive gene, *Lv*ALF was identified, and its function was characterized by RNA interference. *Lv*ALF knockdown resulted in significantly rapid increase of shrimp mortality caused by toxin injection. Protein-protein interaction analysis by molecular docking suggested that *Lv*ALF possibly neutralizes VP_{AHPND} toxin through its LPS-binding domain. The data generated in this study provide preliminary insights into the differences in the immune response of shrimp to the bacterial and toxic aspect of VP_{AHPND} as a disease.

1. Introduction

In 2013, the causative agent of acute hepatopancreatic necrosis disease (AHPND), earlier known as early mortality syndrome (EMS), was identified as *Vibrio parahaemolyticus* [49]. Being ubiquitous in the marine environment, *V. parahaemolyticus* is only considered as an opportunistic pathogen [20]. All AHPND-causing strains of *V. parahaemolyticus* (VP_{AHPND}) that are uniquely virulent to shrimp were found to have a large extra-chromosomal plasmid that is absent in non-AHPND strains [14,18,54]. This AHPND-causing plasmid contains 2 toxin genes named as PirA and PirB because they are homologous to the *Photorhabdus* insect-related (Pir) binary toxin [20,40]. Because the ability to cause disease is lost by experimental deletion or the natural absence of plasmid-encoded toxins, the toxins may be considered as the most important factors of AHPND pathogenesis.

In the early stage of VP_{AHPND} infection, sloughing of the hepatopancreas tubule epithelial cells can be observed in histological analysis, while atrophied pale hepatopancreas, the most common sign of AHPND

* Corresponding author. Center of Excellence for Molecular Biology and Genomics of Shrimp, Department of Biochemistry, Faculty of Science, Chulalongkorn University Omics Science and Bioinformatics Center, Faculty of Science, Chulalongkorn University, Thailand.
E-mail address: kunlaya.s@chula.ac.th (K. Somboonwiwat).
[1] These authors contributed equally to this work.
[2] Current Addresses: National Institute of Molecular Biology and Biotechnology, College of Science, University of the Philippines, Diliman, Quezon City, Philippines; and Philippine Genome Center, University of the Philippines, Diliman, Quezon City, Philippines.

https://doi.org/10.1016/j.fsi.2018.06.054
Received 12 April 2018; Received in revised form 26 June 2018; Accepted 29 June 2018
Available online 18 July 2018

in diseased shrimp, can be observed in the later stages of infection, when necrosis of the hepatopancreas tubule epithelial cells and massive hemocyte infiltration occurs [30,45]. Ref. [20] showed that VP_{AHPND} initially colonizes the stomach and secretes toxins at 6 h post infection (hpi), which would then allow both toxin proteins and, subsequently, bacteria to spread from the stomach to the hepatopancreas at 12-hpi. While this information describes the pathogenesis of the AHPND, the mechanistic processes of the shrimp immune system during infection especially the response to VP_{AHPND} toxins is not yet fully understood. Recent transcriptome analysis in hemocyte *Litopenaeus vannamei* challenged with non-AHPND strains of *V. parahaemolyticus* showed differential expression of immune-related genes induced by *Vibrio* infection [37]. Recently, a study showed that the hemocyanin (HMC) gene family was identified from *L. vannamei* hepatopancreas as up-regulated upon VP_{AHPND} infection. Among the hemocyanin isoforms found, hemocyanin subunit L3 (HMCL3) and hemocyanin subunit L4 (HMCL4) were induced in the hepatopancreas as a response to VP_{AHPND} toxin from 1 to 3 h after injection [6].

The aim of the study is to analyze the expression responses of the shrimp hemocyte transcriptome, which is a major immune tissue related to VP_{AHPND} infection, by RNA sequencing (RNA-seq). The effect of partially purified VP_{AHPND} toxin challenge on selected genes was also revealed by qRT-PCR. This provides preliminary insights into the differences in the immune response of shrimp to the bacterial and toxic aspect of AHPND as a disease. Likewise, the study aims to highlight various roles of genes in different stages of AHPND infection.

2. Materials and methods

2.1. Shrimp samples

Shrimp, weighing about 6–8 g, were obtained from a local shrimp farm. They were acclimatized in rearing tanks with ambient temperature of 30 ± 2 °C, water salinity of 20 parts per thousand, and constant aeration. They were fed with commercial pellets 2 times a day and kept in the rearing tanks for 2 weeks before any experiment or tissue collection.

2.2. VP_{AHPND} and VP_{AHPND} toxin challenge

After acclimatization, shrimp were challenged with VP_{AHPND} Thamai isolates by immersion in tanks that were inoculated by a bacterial suspension to a final concentration of 1.5×10^6 CFU/ml as described by Ref. [6]. VP_{AHPND} was grown on TCBS agar. Several colonies were inoculated in tryptic soy broth (TSB) containing 1.5% NaCl and incubated at 30 °C with 250 rpm shaking overnight. This culture was then inoculated to a fresh TSB with 1.5% NaCl medium in a 1:100 ratio and incubated at 30 °C with 250 rpm shaking until an optical density at 600 nm (OD_{600}) of 2 (approximately 10^8 CFU/mL) was achieved. The median lethal dose (LD_{50}) of bacterial inoculants at 48 h was determined in 10 shrimp.

The partially purified VP_{AHPND} toxin, used for knockdown and challenge experiments, was prepared from crude VP_{AHPND} toxin by ammonium sulfate precipitation and dialysis according to [6]. The partially purified VP_{AHPND} toxin was dissolved and dialyzed against 1 × PBS pH of 7.4, quantified by Bradford protein assay, and checked for the presence of PirAB toxin protein using 15% SDS-PAGE before use in any experiment. The partially purified VP_{AHPND} toxin challenge resulting in AHPND in shrimp was confirmed by observation of morphological changes in the hepatopancreas such as paling and atrophy as well as lethargy in surviving shrimp. The partially purified VP_{AHPND} toxin at the dosage that yields 100% mortality in two days which is 0.2 μg/g shrimp was prepared by diluting toxin in 1 × PBS mixed with a red food-grade dye. The red food-grade dye was used to visualize and make sure that injections were administered properly into the shrimp muscle during injection experiments.

2.3. Next generation sequencing and data analysis

For transcriptome analysis, hemocyte collection was done by drawing approximately 500 μl of hemolymph from the ventral sinus of the shrimp using a sterile syringe with an equal volume of filter sterilized and pre-cooled anticoagulant (MAS solution) as described by Ref. [43]. Hemocytes were immediately collected from the suspension by centrifugation in 800 × g for 10 min at 4 °C and kept in liquid nitrogen. Hemocyte from 10 individuals of VP_{AHPND}-challenged shrimp at each time point (0, 3, 6 and 48 h post challenge) was pooled in triplicates. The hemocyte pool for early phase of infection from the 3-h time point was further mixed with the 6-h time point. Total RNA was extracted using Favorgen Tissue Total RNA mini kit (Biotech Corp.).

Total RNA extracts were analyzed in EtBr-stained 1.2% agarose gel and by Agilent 2100 Bioanalyzer using RNA 6000 Pico Kit (Agilent) to determine the integrity and quality. After RNA concentrations were measured by Qubit® RNA HS Assay Kit (ThermoFisher Scientific) on Qubit® 2.0 flourometer, cDNA libraries from 4 μg total RNA were then constructed following the manufacturer's instruction for TruSeq® stranded mRNA LT sample prep kit (Illumina).

The 3 libraries, 0-h library, 3/6-h library and 48-h library, were sequenced using NextSeq 500 High Output v2 Sequencing Kit (Illumina) in a NextSeq 500 desktop sequencer (Illumina) along with 9 other indexed libraries, which were normalized and pooled with a 1% PhiX control spike-in. Using FastQ Toolkit available through the BaseSpace (Illumina) public app repository, adapter trimming and other quality control filtering of raw reads were performed. High quality reads from the 3 hemocyte libraries (SRR6942061, SRR6942062, SRR6942059), and an additional hepatopancreas library (SRR6942060), were assembled together to form a transcriptome reference in Trinity v2.06 software [13]; from which transcript abundance can be based and estimated using RSEM software that is wrapped by scripts included in Trinity. EdgeR software [38] was used to detect differentially expressed transcripts and genes using a dispersion parameter of 0.3.

Leveraging different software for functional annotation, such as BLAST [2]; PFAM [35]; KEGG [16]; Gene ontology [3] and eggNOG [34]; and then running GO-Seq [56]; the Trinotate workflow (http://trinotate.github.io/) was used to analyze gene ontology enrichment for differentially expressed features. UniProt accession numbers from the Trinotate workflow were mapped into Entrez GeneIDs using the UniProt Retrieve/ID mapping tool (http://www.uniprot.org/uploadlists/). The resulting Entrez GeneIDs were then used in KOBAS 2.0 (http://kobas.cbi.pku.edu.cn/home.do) to map KEGG Orthology or conduct enrichment analysis. The identified KEGG orthologies were used as inputs in KEGG Mapper - Search Pathway tool (http://www.kegg.jp/kegg/tool/map_pathway1.html) for mapping to the reference KEGG Pathways and determine distribution. BLAST2GO [10] was used for supplementary annotation. Supplementary tools from galaxy services [1] of National Center for Genome Analysis Support (https://galaxy.ncgas-trinity.indiana.edu/) and Galaxy Queensland (http://galaxy-qld.genome.edu.au/galaxy) such as Fasta tools, Trinity software, BLAST+ were also used.

2.4. Quantitative real-time PCR analysis

A total of 9 representative transcripts from the reference assembly including anti-lipopolysaccharide factor (*Lv*ALF), crustin p (CRU), serpin 3 (SER), C-type lectin 3 (CTL), clottable protein 2 (CLO), mitogen-activated protein kinase kinase 4 (MKK4), P38 mitogen-activated protein kinase (P38), protein kinase A regulatory subunit 1 (PKA) and DNAJ homolog subfamily C member 1-like (DNJ) were analyzed using quantitative real-time PCR (qRT-PCR) to evaluate and confirm the differential expression profiles reported by RNA-Seq analysis. The shrimp EF-1α gene was used as an internal control. Twelve shrimp were challenged with VP_{AHPND} as previously described. Hemocyte of three

Table 1
List of all primer sequences. Primers were designed using Primer3 packaged in Geneious R6. Classifications are based on [47].

Name	Accession	Name	Sequence (5′to3′)	Tm	Target
qRT-PCR Primers					
EF-1α	GU136229.1	EF-1α-F	CGCAAGAGCGACAACTATGA	58.4	171
		EF-1α-R	TGGCTTCAGGATACCAGTCT	57.8	
Antimicrobial peptides					
anti-lipopolysaccharide factor	DQ208702	ALF (197F)	GCTTCACCGTCAAACCTTACATC	60.1	194
		ALF (389R)	CACCGCTTAGCATCTTGTTCG	59.9	
crustin p	AY488496	CRU (292F)	GTTCCAACGACTACAAGTGTGC	60.0	185
		CRU (476R)	CCAAAACATCGGTCGTTCTTCAG	60.4	
Protease and protease inhibitors					
serpin 3	KM280385	SER (857F)	TAAGGGATCAAGACTCAGCATGG	59.9	175
		SER (1031R)	TACCAGCTCCAGTGACTCTTCTA	60.0	
Pattern recognition receptor proteins					
C-type lectin 3	JQ804930	CTL (369F)	GACTTCGTGGGCACTGATTACTA	60.1	172
		CTL (540R)	GCTTGTAGAAGACGTTGTTCAGC	60.4	
Blood clotting system					
clottable protein 2	EU082133	CLO (782F)	TCCCTTTCACTGTCCTTGAGAAC	60.2	223
		CLO (1004R)	GTGGTGATGCTCAGACTGACTAA	60.1	
Signaling transduction					
mitogen-activated protein kinase kinase 4 (MKK4)	KJ023198	MKK (497F)	GGGAGATTGGAAGAGGAGGTTTT	60.0	206
		MKK (702R)	ACAGTCACCCTCCTTGAATATGG	59.8	
P38 mitogen-activated protein kinase	JN035902	P38 (585F)	AGATTGTGAGCTGAAGATCCTCG	60.2	152
		P38 (736R)	AGCCTACTGACCAGATATCCACT	60.1	
protein kinase A regulatory subunit 1	KT203799	PKA (105F)	GCTTGAACCAGTGTCCATAGAGT	60.3	167
		PKA (271R)	CACCAAAGTAGTCTGAAGTCCCA	59.9	
Heat shock proteins					
DNAJ homolog subfamily C member 1-like	XM_014358733	DNJ (436F)	GTCCCTTCAGCTTCATCCAGATA	59.6	161
		DNJ (596R)	AGTATATAGGAGAGCGCCAGTCA	60.2	
Gene Knockdown Primers					
*Lv*ALF-AVR_F	CGTGTCTCTGTGTTGACAAG				56.7
*Lv*ALF-AVR_R	CCTTGTAGTTCAGCTGTAACC				56.3
T7_*Lv*ALF-AVR_F	GGATCCTAATACGACTCACTATAGG-CGTGTCTCTGTGTTGACAAG				68.0
T7_*Lv*ALF-AVR_R	GGATCCTAATACGACTCACTATAGG-CCTTGTAGTTCAGCTGTAACC				68.0
GFP-T7-F	GGATCCTAATACGACTCACTATAGG-ATGGTGAGCAAGGGGGAGGA				68.0
GFP-T7-R	GGATCCTAATACGACTCACTATAGG-TTACTTGTACAGCTCGTCCA				67.0
GFP-F	ATGGTGAGCAAGGGGGAGGA				62.8
GFP-R	TTACTTGTACAGCTCGTCCA				56.2

VP_{AHPND}-infected shrimp was collected at 0-hpi, 3-hpi, 6-hpi, and 48-hpi. Total RNA was isolated using FavorPrep™ Tissue Total RNA Mini Kit (Favorgen Biotech Corp.) and then, first strand cDNA was synthesized using 1 μg total RNA in a reaction containing 1 mM dNTP, 10 units of RNase inhibitor, 0.5 μM oligo-dT (Promega), 1 × RevertUP buffer (BiotechRabbit), and 100 units of RevertUP Reverse Transcriptase (BiotechRabbit).

To study the effect of VP_{AHPND} toxin on the expression of genes under study, shrimp were divided into an experimental and a control group, containing a sample size of 20 individuals. They were intramuscularly injected with 1 × PBS, pH 7.4 and 0.2 μg/g per shrimp of partially purified VP_{AHPND} toxin containing 1% red colored food-grade dye (Winner, Thailand), respectively. Then, the hemocyte of three shrimp from each group was collected at 0, 1, 3, 12, and 24 h post-injection (hpi). Total RNAs and cDNAs were prepared as above.

Gene specific primers (Table 1) were designed from the sequences obtained from RNA-seq data by Primer3 [50] as packaged in Geneious R6 (Biomatters, Ltd). The qRT-PCR reactions, which were composed of 10-fold diluted cDNA template, 1x QPCR Green Master Mix (LRox) (BiotechRabbit) and 0.5 or 0.25 μM forward and reverse primers, were run in CFX96 Touch™ Real-time PCR system (Bio-Rad). Relative expression of each gene was determined and analyzed according to ref. [32] using EF-1α as the control gene. The control was assigned as the 0-hpi group for the bacterial challenge experiment or the 0-h PBS-injected group for the partially purified VP_{AHPND} toxin challenge experiment. Statistical analyses such as one-way ANOVA and Dunnett's multiple comparisons test were conducted in Prism version 6 (GraphPad).

2.5. *LvALF* gene knockdown by RNA interference

The *Lv*ALF dsRNA was prepared using cDNA from *L. vannamei* hemocyte as a template for producing sense and anti-sense DNA templates of *in vitro* transcription. DNA templates (sense and anti-sense strands) containing the T7 promoter sequence at the 5′-end were generated by PCR using *Lv*ALF-T7-F and *Lv*ALF-R primers for the sense strand template, and the other with *Lv*ALF-F and *Lv*ALF-T7-R primers (Table 1). The dsRNA was prepared using T7 RiboMAX™ Express RNAi System (Promega).

L. vannamei samples (approximately 3 g body weight) were divided into three groups of three individuals each. One control group was injected with 10 μg of GFP dsRNA per g of shrimp weight, and another with 0.85% NaCl. The experimental group was injected with 10 μg of *Lv*ALF-dsRNA per gram of shrimp weight. Hemocyte of individual shrimp was collected at 16 h post dsRNA injection and total RNA was extracted, treated with RNase-free DNaseI. An equal amount of DNA-free total RNA from three shrimp was pooled, and 1 μg of pooled total RNA was used for the first strand cDNA synthesis using the RevertAid First Strand cDNA Synthesis kit (Fermentas). *Lv*ALF gene expression was analyzed by RT-PCR using *Lv*ALF-AVR_F/R primers (Table 1) to confirm efficiency of *Lv*ALF gene knockdown. The EF-1α gene was amplified, as an internal control, using the EF-1α-F/R primer pair (Table 1). The PCR conditions were 94 °C for 1 min, followed by 28 cycles (for EF-1α) or 26 cycles (for *Lv*ALF) of 95 °C for 30 s, 58 °C for 30 s, and 72 °C for 30 s, and then a final extension at 72 °C for 5 min. The PCR products were analyzed by 1.5% (w/v) agarose gel electrophoresis.

2.6. Cumulative mortality assay upon VP_{AHPND}-toxin challenge of LvALF-knockdown shrimp

The percentage cumulative mortality was investigated in *Lv*ALF-knockdown shrimp after VP_{AHPND} toxin injection. Twenty *L. vannamei* shrimp of approximately 3 g body weight per group were injected with *Lv*ALF-dsRNA, GFP-dsRNA or 0.85% NaCl as above. Diluted VP_{AHPND} toxin solution at a dosage that causes 100% mortality of shrimp in 2 days post injection was intramuscularly injected into the respective group of shrimp. Mortality was observed every 1 h after VP_{AHPND} toxin injection for 24 h.

2.7. Molecular modeling, model validation and molecular docking

In *L. vannamei*, several sub-isoforms of *Lv*ALF containing single amino acid polymorphisms have been found in the NCBI GenBank database such as *Lv*ALF AV-R (accession no. ABB22832), *Lv*ALF AV-K (accession no. ACT21197), *Lv*ALF AA-K (accession no. ABB22833) and *Lv*ALF VV-R (accession no. ABB22836) (https://www.ncbi.nlm.nih.gov/). To predict the protein-protein interaction of *Lv*ALF and VP_{AHPND} toxin proteins, PirA & PirB, and each of the different *Lv*ALF isoforms were submitted to I-TASSER server [59]; a protein prediction software that is based on model building using multiple-template fragment alignments to build-up predicted-3D structures. The *Lv*ALF model with lowest root-mean-square deviation value (RMSD) was used for further analysis. Stereochemistry of all the models was evaluated by Ramachandran Plot Analysis (http://mordred.bioc.cam.ac.uk/~rapper/rampage.php). The 3D structures of PirA (PDB ID. 3X0T) and PirB (PDB ID. 3X0U) in VP_{AHPND} toxin complex reported by ref. [21] were retrieved from Protein Data Bank (http://www.rcsb.org/). All of ionizable amino acid residues in predicted models were protonated at pH 7.4 by using H++ 1.0 software (http://biophysics.cs.vt.edu/). Molecular docking was performed by web-based service ClusPro [9] to identify the interaction between each *Lv*ALF and VP_{AHPND} toxin proteins. Swiss PDB viewer [5] and VMD [15] were used to perform visualization of 3D models. The coefficient weights of protein binding was calculated from $E = 0.40E_{rep} + (-0.40)E_{att} + 600E_{elec} + 1.00E_{DARS}$ [19].

3. Results

3.1. De novo assembly and annotation

The cDNA libraries from hemocytes of *L. vannamei* challenged with AHPND-causing strain of *V. parahaemolyticus* at 0-hpi, 3/6-hpi, and 48-hpi were sequenced on a high throughput sequencing system, NextSeq 500 (Illumina). The NextSeq 500 run generated a total of 125, 587, 193 raw reads across 3 different libraries which had an average read count of 41 million reads. Quality control and filtering produced 125, 401, 257 clean reads (99.85% retention), which were used in the subsequent Trinity assembly. Assembly statistics are shown in Table 2, where a total of 127,205 transcripts and 104,233 putative genes, with sequence lengths ranging from 201 to 16,976 bp, and an N50 transcript length of 1360 base pairs (bp) have been listed. Sequencing reads were deposited into the Short Read Archive (SRA) of the National Center for Biotechnology Information (NCBI) and can be accessed using accession number SRP137285. All transcripts from the reference assembly were searched against the SwissProt database using BLASTx, which reported that 78% had significant hits (E-value $\leq 10^{-1}$). All sequences with specific hits to the database were graphed and the organisms represented in the library (Fig. 1A) are *Homo sapiens* (12.58%), *Mus musculus* (10.72%), *Drosophila melanogaster* (5.75%), *Arabidopsis thaliana* (4.32%), *Rattus norvegicus* (3.49%), *Bos taurus* (2.59%), etc.

Table 2
Statistics for NGS sequences.

Number of Filtered Reads per Library	
0-hpi library	39,755,956
3/6-hpi library	47,217,902
48-hpi library	38,427,399
Statistics for numbers of transcripts:	
Number of transcripts:	127,205
Total trinity 'genes'	104,233
Number of transcripts ≥ > =1 kb:	22,412
Number of transcripts in N50:	16,467
Number of bases in all transcripts	92,165,807
Number of bases in contigs ≥ > =1 kb	53,012,218
Percent GC:	43.75
Statistics for transcript lengths:	
Min transcript length:	201
Max transcript length:	16,976
Median transcript length:	350
N50 transcript length:	1360

Distribution of 11,952 transcripts with hits to Gene Ontology as leveraged by GO-seq in the Trinity package is shown in Fig. 1B for a total of 52 GO terms in 3 ontologies. Meanwhile, 10,745 KEGG orthologies were assigned to the query sequences, where Metabolic Pathways is the highest assigned KEGG reference pathway (Fig. 1C). A protein BLAST was also done by using predicted coding sequences from the Trinotate protocol and these annotations, along with PFAM information, are shown in Supplementary Table 1.

3.2. Identification of differentially expressed transcripts

A gene was considered differentially expressed when the absolute value of $\log_2$ ratio of that gene in the control (0-hpi) and experimental (3/6-hpi and 48-hpi) libraries is greater than or equal to 1.5 ($|\log_2(a/b)| \geq 1.5$) at a significance of $P \leq 0.001$. Using this criterion in gene expression analysis by edgeR, 815 differentially expressed transcripts were detected in the 0-hpi vs 3/6-hpi libraries at a fold-change of at least 2.8 ($2^{1.5}$). Of these transcripts, 430 are significantly up-regulated in the 3/6-hpi library. 351 (82%) had alignments to Genbank SwissProt sequences as reported by BLASTx. In the 0-hpi vs 48-hpi libraries, 1067 transcripts are at least 2-fold differentially expressed at a significance of $P \leq 0.001$, where 537 transcripts are up-regulated in the 48-hpi library. 446 (83%) of these up-regulated genes had significant alignments to Genbank SwissProt sequences as reported by BLASTx. 202 genes were found to be up-regulated in both 3/6-hpi and 48-hpi libraries. Differentially expressed genes in the 3/6-hpi and 48-hpi library were listed in Supplementary Tables 2 and 3. All the differentially expressed genes were also clustered in a hierarchical heatmap where expression values are reported as (TMM-normalized) FPKM expression values. This heat map is showed in Fig. 2 where major expression clusters are supported by tree percentage values.

3.3. Expression analysis of VP_{AHPND}- and VP_{AHPND} toxin-responsive genes in shrimp hemocyte

In this experiment, pale and atrophied hepatonpancreas was observed in all VP_{AHPND} challenged shrimp that were sampled confirming AHPND pathogenesis. Nine genes were specifically chosen for quantitative real-time PCR analysis to evaluate the expression profiles reported by the RNA-Seq analysis and explore changes in the expression of possibly interesting genes from *in vivo* data. These genes are: crustin p (CRU), anti-lipopolysaccharide factor AV-R isoform (*Lv*ALF), serpin 3 (SER), c-type lectin 3 (CTL), clottable protein 2 (CLO), mitogen-activated kinase kinase 4 (MKK4), p38 mitogen-activated protein kinase

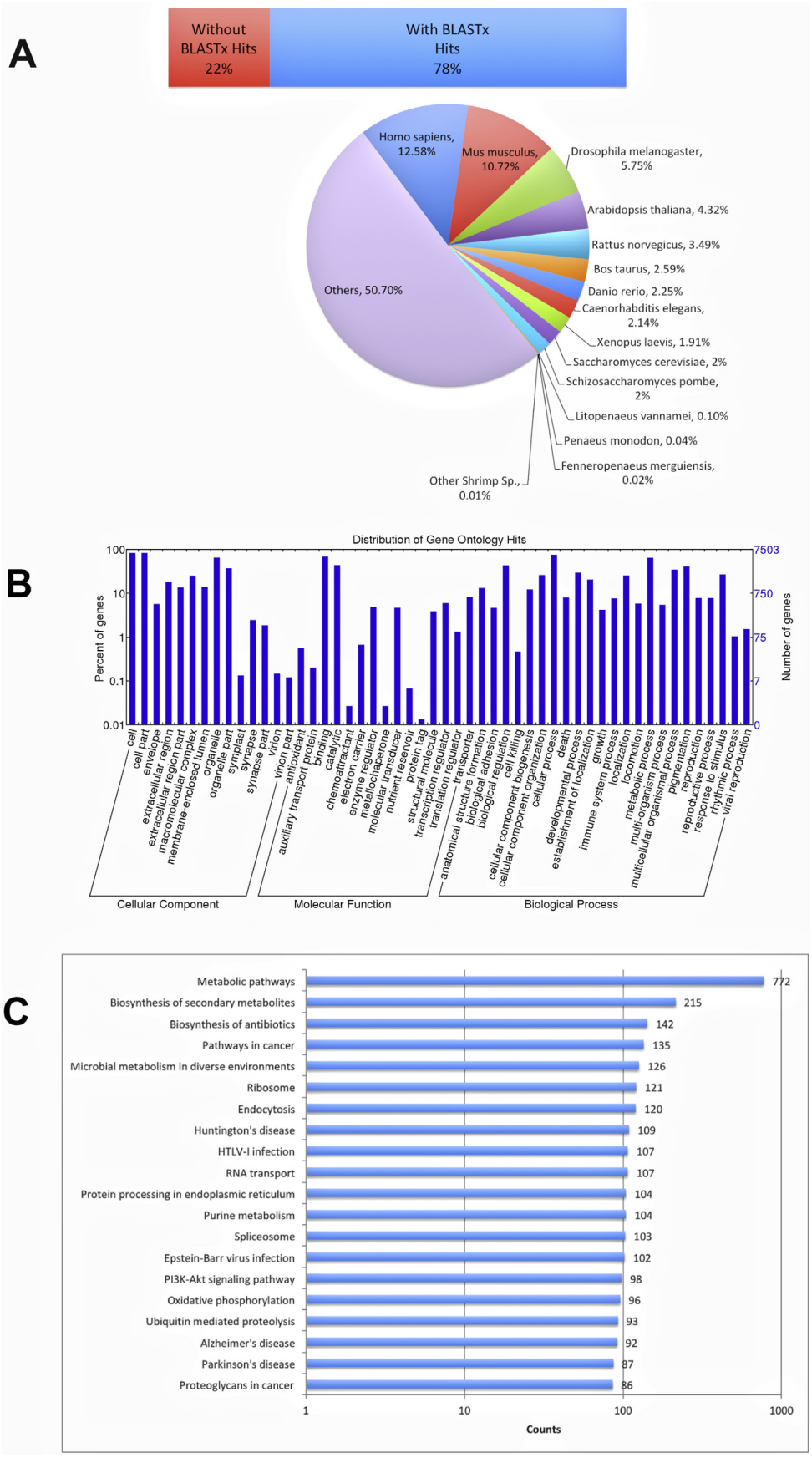

Fig. 1. Annotation of *Litopenaeus vannamei* transcriptome unigenes. A. Percentage of sequences in the transcriptome library aligned against SwissProt Database with E-values of ≤ 10 and organisms represented in the assembly; **B.** Distribution of Gene Ontologies represented in the transcriptome assembly; **C.** Distribution of top 20 KEGG pathways represented in the library.

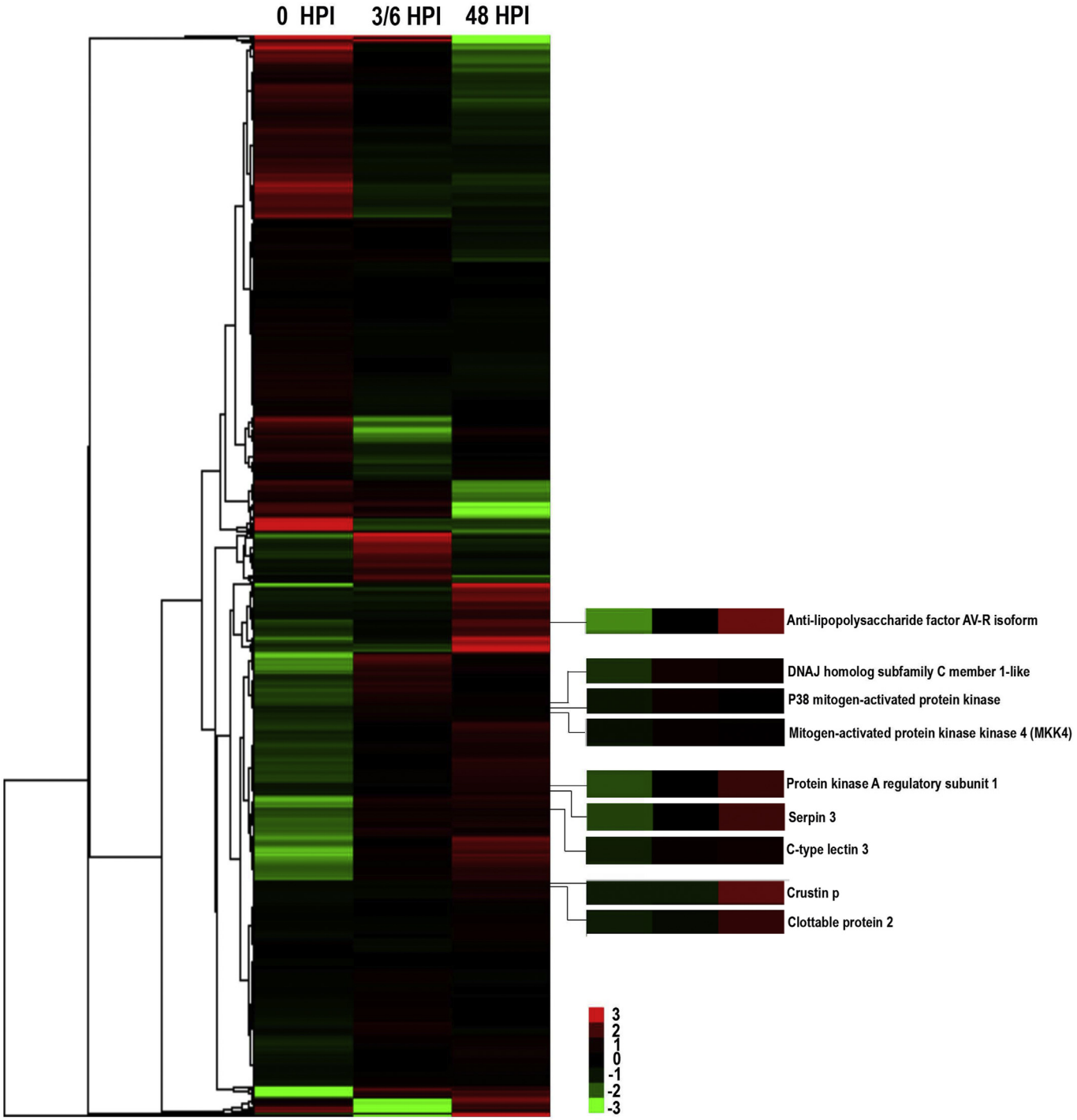

Fig. 2. Hierarchy-clustered heatmap of (TMM-normalized) FPKM expression values for those features that are at least 2-fold differentially expressed and *P*-value < 0.0001.

(P38), protein kinase A regulatory subunit 1 (PKA), and DNAJ homolog subfamily C member 1-like (DNJ). Out of the 9 tested, the expressions of 8 genes were significantly different from that of the 0-h control group in at least one time point after challenge (Fig. 3). Specifically, the expression patterns of 5 genes from RNA-Seq were confirmed to be similar to the qRT-PCR expression profiles in VP_{AHPND}-challenged group. The expression of these same 9 genes was tested in shrimp challenged with partially purified VP_{AHPND} toxin. Using PBS-injected shrimp as the control group, we found that 5 genes were differentially expressed in at least one time point with a cut-off $P < 0.01$ (Fig. 3). Out of these, 3 genes, CRU, SER and p38 were down-regulated while 2 of them, *Lv*ALF and CTL were up-regulated upon VP_{AHPND} toxin challenge. Looking at both bacterial and toxin challenges, the expression levels of *Lv*ALF and CTL were up-regulated, although only that of CTL was statistically significant.

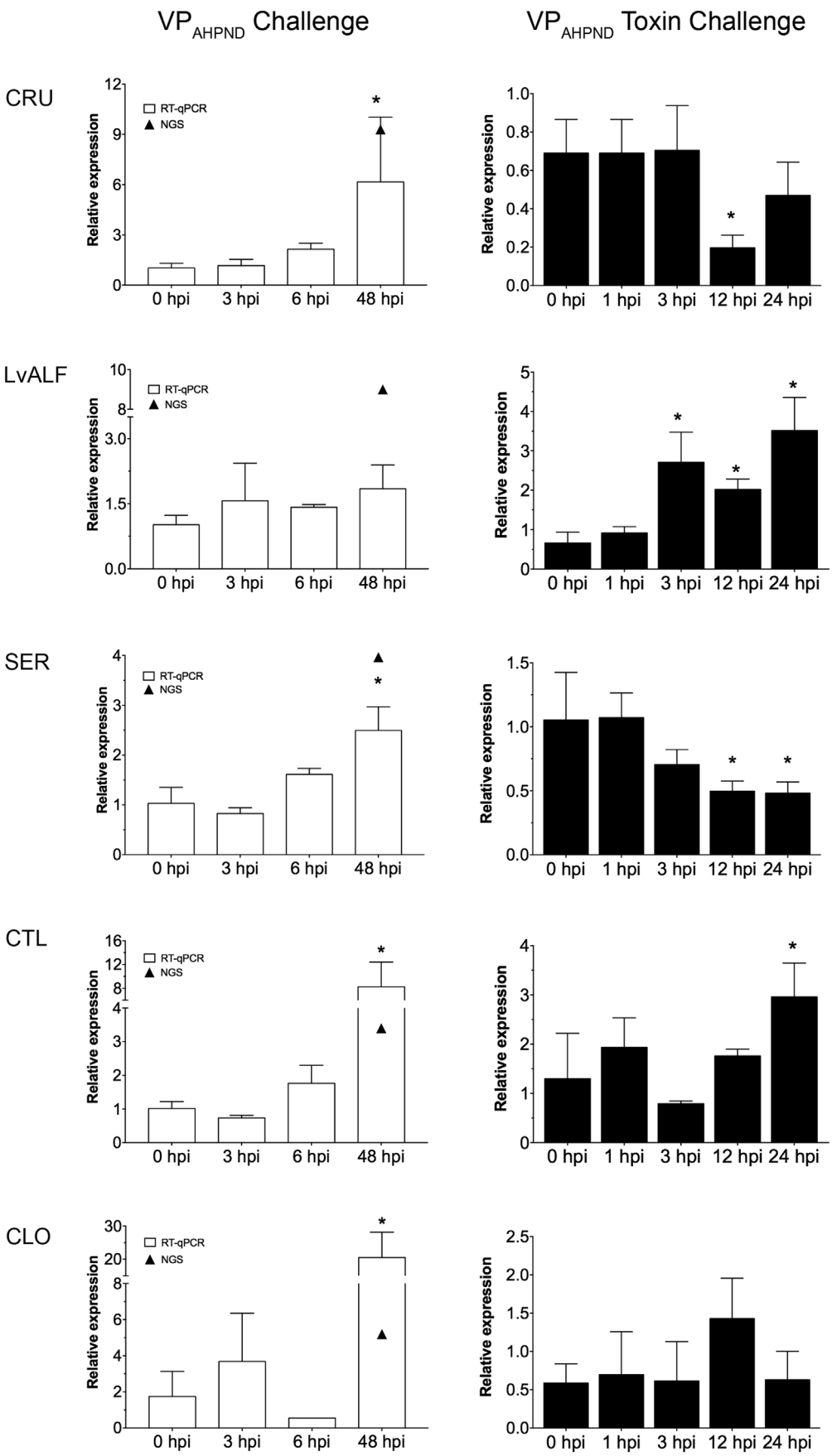
VP AHPND Challenge
VP AHPND Toxin Challenge
CRU
LvALF
SER
CTL
CLO
RT-qPCR
NGS
Relative expression
0 hpi
3 hpi
6 hpi
48 hpi
1 hpi
12 hpi
24 hpi

Fig. 3. Expression analysis of representative up-regulated genes by qPCR. Nine up-regulated genes (CRU –crustin p; *Lv*ALF –anti-lipopolysaccharide factor; SER –serpin 3; CTL –C-type lectin 3; CLO –clottable protein 2; MKK4–mitogen-activated protein kinase kinase 4; P38 –p38 mitogen-activated protein kinase; PKA–protein kinase A regulatory subunit 1; DNJ –DNAJ homolog subfamily C member 1-like) were analyzed for the expression in hemocyte of VP_{AHPND} and VP_{AHPND} toxin -challenged *L. vannamei* at various time points by qPCR using EF-1α as the internal control gene. Asterisks indicate significant difference ($P < 0.05$) from the respective 0 h sampling group based on Dunnett's multiple comparisons test. Triangles indicate expression values with statistical significance from RNA-Seq data analaysis, where expression in 3/6 libraries is plotted in between the 3-hpi and 6-hpi categories of the qPCR counterpart. Absence of these triangles for a gene indicates no significant difference between the specific time point/library and the control.

3.4. Effect of VP_{AHPND} toxin injection on survival of LvALF-knockdown shrimp experiments

According to the expression profiles reported in this study, expression of *Lv*ALF gene was up-regulated upon VP_{AHPND} toxin challenge but showed no significant change upon VP_{AHPND} challenge raising the question on its function during VP_{AHPND} infection. In this experiment, we further explored if *Lv*ALF has an immune role during toxin exposure in shrimp by determination of survival of *Lv*ALF-knockdown shrimp upon toxin challenge. From our observation, all groups that were injected with partially purified VP_{AHPND} toxin reached 80–90% mortality in 24 h, while all control groups without toxin injection survived (Fig. 4B). The test group, where *Lv*ALF gene knockdown was successful (Fig. 4A), reached 100% mortality in as early as 9 h post VP_{AHPND} toxin injection.

3.5. Prediction of LvALF/VP_{AHPND} toxin interaction by molecular modeling and docking

Computational analysis based on the availability of ALF*Pm*3 protein from shrimp *Penaeus monodon* and VP_{AHPND} toxin structures in PDB database was done using molecular docking of shrimp ALFs with the toxin. Due to *Lv*ALF containing several sub-isoforms that arise from amino acid polymorphism, the predicted 3D structure models of each *Lv*ALF protein sub-isoform including *Lv*ALF AV-R, *Lv*ALF AV-K, *Lv*ALF VV-R, and *Lv*ALF AA-K were constructed by web-server I-TASSER software. The results showed that the 3D structure of *Lv*ALF proteins were structurally similar to the NMR structure of ALF*Pm*3 (Fig. 5A). The RMSD value between the Cα atom of the template ALF*Pm*3 and *Lv*ALF AV-R, *Lv*ALF AV-K, *Lv*ALF VV-R, and *Lv*ALF AA-K was 0.73, 0.70, 0.64 and 0.59 Å, respectively. Our analysis showed that 90.8%, 95.8%, 95.0% and 96.7% residues of *Lv*ALF AV-R, *Lv*ALF AV-K, *Lv*ALF VV-R and *Lv*ALF AA-K were in the most favorable region, while 9.2%, 4.2%, 5.0% and 3.3% residues were in the allowed region, respectively. ClusPro web-based software was used to analyze the interaction of *Lv*ALF and VP_{AHPND} toxin protein. Molecular modeling and docking analysis suggests that *Lv*ALF AV-R, *Lv*ALF AV-K, *Lv*ALF VV-R and *Lv*ALF AA-K could interact with the PirB protein of VP_{AHPND} toxin through their LPS-binding sites (Fig. 5B). The coefficient weights of the lowest energy of each interaction were −1176.1, −965.9, −1113.3 and −1162.5, respectively.

4. Discussion

AHPND, or acute hepatopancreatic necrosis disease, is known to be caused by strains of *Vibrio parahaemolyticus*, which accumulates in the stomach and secretes PirA/B in the hepatopancreas [20]. The mechanism by which VP_{AHPND} kills shrimp is currently believed to be caused by the toxin damaging the shrimp stomach epithelium, causing further spread of the toxin proteins together with the bacteria into the hepatopancreas and leading to sloughing of the hepatopancreatic tubule epithelial cells. While this information on the pathogenesis of VP_{AHPND} in the shrimp tissues exists, the mechanistic responses of the shrimp immune system related to the histological events are yet to be understood. Preliminary data in VP_{AHPND} infection studies showed that genes of Toll and IMD pathways and their downstream antimicrobial peptides (AMPs), such as penaeidins, anti-lipopolysaccharide factor, crustin and lysozyme, are overexpressed in the hepatopancreas [55]. Such an observation is expected because the hepatopancreas is one of the major AHPND targets [20]. Meanwhile, data on the expression of the said genes in the stomach and the hemocytes showed that they are suppressed [55]. This is an interesting observation because the hemocytes are also well-known as major immune organs of shrimp [22]. In a recent paper exploring the hemocyte transcriptome of Pacific white shrimp (*L. vannamei*) challenged by *Vibrio parahaemolyticus*, five genes from the humoral immunity such as MNK1/2 MAP kinase interacting serine (MNK), C-type lectin 3 (CTL3), 179 scavenger receptor B1 (SR), gamma-interferon-inducible lysosomal thiol reductase 180 (GILT), and anti-lipopolysaccharide factor-like protein (ALFP) were shown to be significantly up-regulated and important in bacterial clearance [37]. This highlights the diversity of novel genes found shrimp that are crucial during a bacterial infection.

In this study, the gene expression of crustin p is about 6-fold up-regulated while *Lv*ALF did not significantly change based on the qRT-PCR. Crustin molecules are produced and stored in hemocyte granules and thus are easily induced by microbial stimulation. They are then released by degranulation into the hemolymph effectively fighting against a broad spectrum of bacteria [4]. As expected, the bacterial challenge experiment showed gene upregulation and the putative release of crustin, together with other anti-microbial peptides such as serpin 3, clottable protein and c-type lectins (Fig. 3). This mechanism highlights the so-called hallmark of shrimp immunity where different antimicrobial peptides and immune molecules are released to fight off bacteria such as $VP_{AHPND.}$ Meanwhile, it is interesting to note that the differences in expression profiles between the other studies may be due to differences in crustin isoforms [46] as well as anti-lipopolysaccharide factor isoforms [12] or bacterial doses used. In our experiments involving challenge with partially purified VP_{AHPND} toxins, we observed that crustin p expression was significantly lower than the PBS-injected control at 12-hpi (Fig. 3), a similar observation with the study by ref. [55]. In these observations, the toxins might have caused significant cellular stress that affected the expression of some genes in the shrimp immune system such as antimicrobial peptides. Apparently, the marked decrease of antimicrobial peptides like ALF, crustin, lysozyme, and penaeidin in response to stresses such as presence of ammonia in water is common in invertebrates at 6 h post exposure [7,57].

Other well-known innate immunity molecules for bacterial infection such as serpin 3 [24,60]; c-type lectin 3 [27,52]; and clottable protein 2 [28] have agreeing data in both RNA-seq and qRT-PCR analysis, which showed significantly up-regulated expressions during VP_{AHPND} challenge (Fig. 3). These genes are well characterized in other shrimp species as mainly detected in hemocytes, induced by and play critical roles in bacterial infection. More specifically, serpins were found to protect their hosts from infection by pathogens or parasites through inhibiting fungal or bacterial proteinases or regulating endogenous proteinases involved in coagulation, proPO activation, or cytokine activation [17,25,26,44,53]. In *L. vannamei*, two serpins, serpin 3 and serpin 8, have been identified and they were both implicated [25,26] as

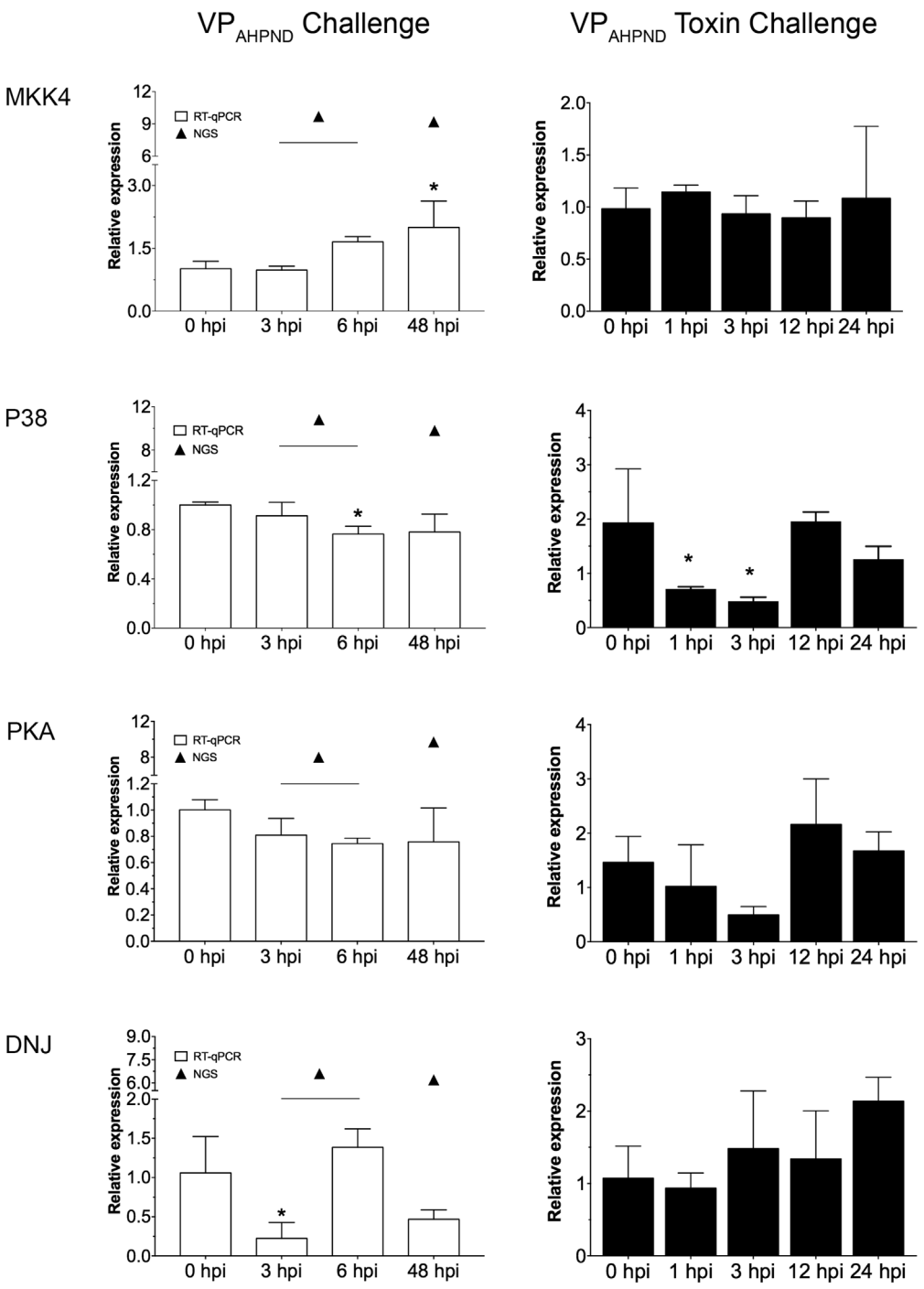

Fig. 3. (*continued*)

important factors during bacterial infection by inhibiting growth of bacteria such as *Vibrio anguillarum*. As the expression of serpin 3 agrees with the expression patterns presented in other studies, this study supports serpin 3 as an important aspect of shrimp immunity during bacterial infection such as VP_{AHPND}.

Likewise, gene upregulation of clottable protein in this study indicates a functional role of the gene during VP_{AHPND} infection. In another study, silencing of clottable protein and its upstream regulator, transglutaminase, showed significantly higher mortalities after bacterial challenge [28].

In qPCR analysis of partial purified VP_{AHPND} toxin-challenged samples, serpin 3 was significantly lower than the control group similar with crustin p. The difference in expression profiles of serpin 3 shows the variability of its response, whether to VP_{AHPND} toxin and bacterial challenges. This phenomenon is also seen in a Chinese shrimp serpin, which is up-regulated after *V. anguillarum* challenge and down-regulated after white spot syndrome virus challenge. Based on this information, a duality of AHPND pathogenesis in terms of the effects of the toxin e.g. cellular stress, or the presence of bacteria on the shrimp immune response may exist.

Meanwhile, up-regulated expression of c-type lectin 3 in both bacteria and toxin -challenged shrimp was observed (Fig. 3). Up-regulation during bacterial challenge was expected because c-type lectins are well-known immune molecules for discrimination of non-self molecules after binding to invading microorganisms [51]. Knockdown of c-type lectin 3 in Pacific white shrimp showing increased bacterial counts in the

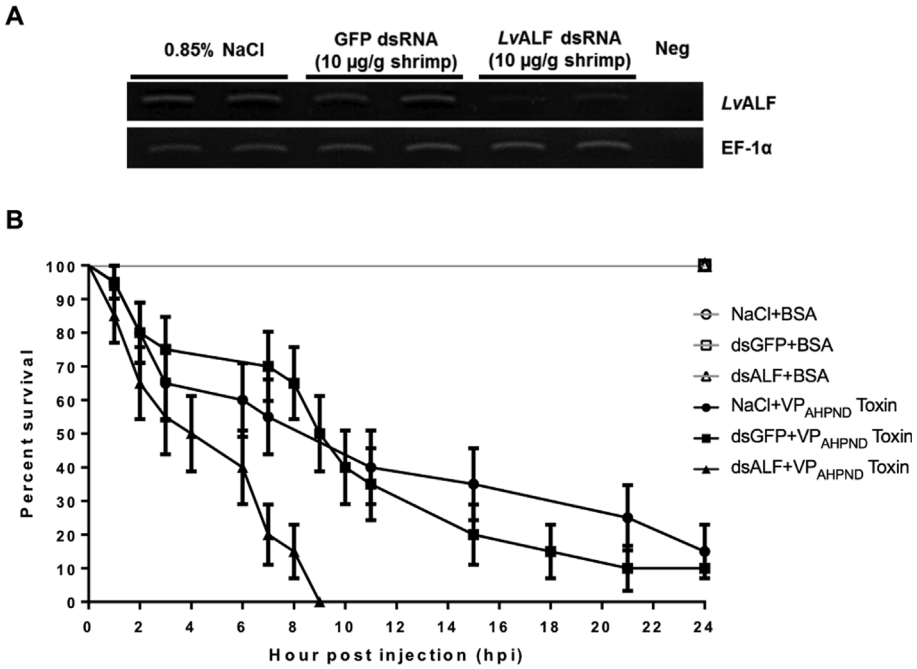

Fig. 4. Survival curve of shrimp during VP_{AHPND} toxin challenge with successful *Lv*ALF gene knockdown. A. Confirmation of *Lv*ALF gene knockdown in *L. vannamei*. Expression level of *Lv*ALF gene in hemocyte of shrimp injected with 0.85% NaCl, 10 µg/g shrimp of GFP dsRNA, and 10 µg/g shrimp of *Lv*ALF dsRNA was determined by semi-quantitative RT-PCR. The 1.5% agarose gel profile was analyzed for the success of *Lv*ALF gene knockdown. Neg is negative control reaction; **B.** Percent survival of shrimp with different injections as indicated by data labels. Standard errors of the survival from 20 individuals are presented as error bars in each time point.

shrimp hemolymph after challenge [37] indicated the crucial role of c-type lectin 3 in bacterial clearance after infection. While the magnitude of the expression of c-type lectin 3 gene is significantly higher in the bacterial challenge experiment than the VP_{AHPND} toxin challenge, up-regulation is detected in both groups, in which the expression profile of bacteria–challenged group is also correctly determined by RNA-Seq data. Aside from binding microorganisms, c-type lectins may induce phagocytosis, prophenoloxidase activating system, respiratory burst, and antiviral immunity [51]. In this study, the described mechanism of c-type lectin in innate immunity is observed in both bacteria and partially purified VP_{AHPND} toxin challenges indicating the important position of lectins in delaying/decreasing morbidity of a wide array of diseases and stress factors in shrimp farms, especially VP_{AHPND} infection.

The shrimp homolog of mitogen-activated protein kinase kinase 4 (MKK4) was also significantly up-regulated in VP_{AHPND}-challenged shrimp (Fig. 3). In the VP_{AHPND} toxin experiment, however, MKK4 expression showed no significant difference from the control. This indicates the possible role of MKK4 in the shrimp immune response for bacteria. In mice, MKK4 becomes activated during cell response to stresses and pro-inflammatory cytokines, which then activates a gene called stress-activated protein kinase-1c (also known as JNK1). The JNK pathway, together with the p38 pathway, are also known as Stress Activated Protein Kinase (SAPK) pathways, since they are activated in response to cellular stress such as irradiation, heat shock, osmotic imbalance, DNA damage, the bacterial product lipopolysaccharide (LPS) as well as inflammatory cytokines [11]. It is possible that the proliferation of bacteria in the gut and in the hepatopancreas caused the up-regulation of the shrimp homolog of MKK4 by signaling cascades activated by LPS. On the other hand, the shrimp homolog of P38 mitogen-activated protein kinase (MAPK) did not show any change in gene expression across all time points in the bacterial challenge. In humans, p38 MAPK, Erk1, and Erk2 phosphorylate and activate MNK1/2 MAP kinase interacting serine (MNK) [36]. The shrimp homolog of MNK1/2 MAP kinase interacting serine (MNK) was associated with bacterial clearance by its up-regulated gene expression during *V. parahaemolyticus* infection and the increased mortality observed in shrimp after its gene knockdown [37]. While the expression of p38 MAPK in this study, along with information from related literature, does not support a conclusive role during bacterial infection, significant changes in p38 MAPK's expression in the 1-h and 3-h time points of this study's toxin-challenge experiments indicate its probable role in the toxin aspect of AHPND pathogenesis. Meanwhile, the difference in expression patterns of MKK4 and p38 MAPK supports the current literature discussing their contrasting involvement in their respective pathways [8]. This then, highlights that the role of p38 MAPK is putatively at the later stages of AHPND when bacteria have already invaded the hepatopancreas and secreted significant amounts of toxin.

Meanwhile, temporal changes in gene expression of the *Lv*ALF in VP_{AHND} challenge were not statistically significant as reported by qPCR. This raises the question on its function in VP_{AHPND} infection because ALFs are known to exhibit antimicrobial activity in shrimp [39,58]. In the VP_{AHPND} toxin-challenged group however, *Lv*ALF was found significantly up-regulated as early as 3 h (Fig. 3). Mapping of the *Lv*ALF AV-R isoform primers for qRT-PCR analysis to different ALF isoforms in *L. vannamei* showed 100% alignment to all the sequences indicating that the expression patterns detected may be the overall response of all *Lv*ALF sub-isoforms mentioned earlier in *L. vannamei*. We thus, consider this possibility and the reason why no significant changes were detected in the bacterial challenge albeit ALFs being well-known antibacterial peptides in *P. monodon* [41]. Although structure prediction of *Lv*ALFs and NMR imaging of ALF*Pm*3 showed similarities in their structures and RMSD values between the Cα atom, previous literature has verified that ALFs are responsive to different pathogen challenges and exhibit multiple antimicrobial and antiviral activities [23,29,48]. It is probable that the various responses of different *Lv*ALF sub-isoforms are masking each other resulting to qRT-PCR not detecting any significant change.

As evidenced by its up-regulation in the toxin injection experiments, *Lv*ALF may have a functional role in preventing cellular toxicity brought by $VP_{AHPND.}$ This role is also supported by knockdown experiments showing that the expression of *Lv*ALF is important in delaying the mortality of shrimp after toxin injection. It is interesting to note that at 9-h post VP_{AHPND} toxin challenge, when the experimental *Lv*ALF knocked-down group reach 100% mortality, shrimp in the VP_{AHPND} toxin-challenged control groups (NaCl + VP_{AHPND} Toxin and dsGFP + VP_{AHPND} Toxin) showed 50% survival, highlighting how decrease/loss of expression of *Lv*ALF aggravates mortality in toxin challenge. This result indicated that *Lv*ALF might play a significant role in protecting shrimp against VP_{AHPND} toxin during infection. In this context, we hypothesize the toxin neutralization mechanism as a function

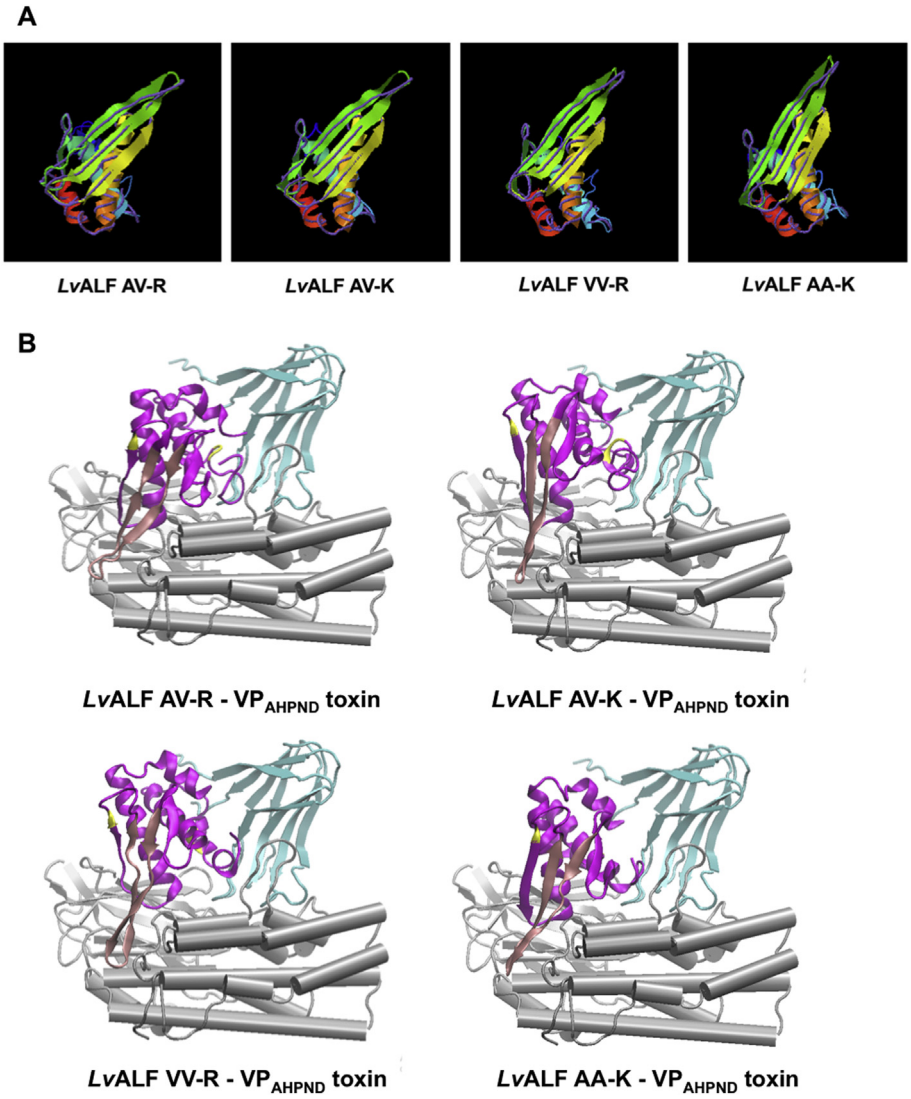

Fig. 5. The molecular modeling and docking analysis for *Lv*ALF and VP_{AHPND} toxin interaction. **A.** The 3D structure alignment of ALF*Pm*3 (line) and *Lv*ALFs (ribbon) including *Lv*ALF AV-R, *Lv*ALF AV-K, *Lv*ALF VV-R and *Lv*ALF AA-K; **B.** Molecular docking of each *Lv*ALF sub-isoform and VP_{AHPND} toxin. The gray color shows PirB protein, blue color shows PirA protein, purple color shows *Lv*ALFs protein, pink color shows LPS-binding site of *Lv*ALFs and yellow color shows the difference amino acid residues of *Lv*ALF isoforms. (For interpretation of the references to color in this figure legend, the reader is referred to the Web version of this article.)

of *Lv*ALF's LPS-binding domain to bind to molecular targets such as the PirA and PirB toxins. After all, this functional domain has been considered a key feature responsible for binding to lipopolysaccharide (LPS) and lipoteichoic acid (LTA) on the bacterial cell membrane [42] and WSSV structural proteins [29]. As seen in the protein model prediction (Fig. 5), the LPS-binding domain protrudes from the surface and is therefore, readily available for binding to any component protein of the VP_{AHPND} toxin. Protein interaction prediction using molecular docking showed low coefficient weights of the lowest energy in a magnitude of −1000 thus suggesting that interaction between *Lv*ALF and VP_{AHPND} toxin is possible through binding of *Lv*ALF's LPS-binding site to the PirB protein of VP_{AHPND} toxin. Toxin neutralization of proteins in shrimp has been recently described [6]; where hemocyanin directly interacts with PirA as reported by protein-protein interaction analysis in ELISA. This mode of shrimp immunity by *Lv*ALF, where the LPS-binding site of *Lv*ALF binds to PirB of the VP_{AHPND} toxin, will be interesting to explore in future studies because a recent report about a natural VP_{AHPND} PirA-B+ mutant that kills shrimp but produces no VP_{AHPND} toxin or AHPND lesions [33] poses the importance of developing new ways to understand and combat the disease not only in terms of exploring the host immune system for battling bacterial infection but also for neutralizing the products bacteria produce.

The shrimp homolog of protein kinase A regulatory subunit 1 showed no significant change in both the bacterial challenge and toxin challenge experiments (Fig. 3). Meanwhile, the DNAJ homolog subfamily C member 1-like was significantly down-regulated in the bacterial challenge at 3-hpi unlike in the toxin challenge, where no significant change was observed (Fig. 3). This quick response in DNAJ at 3-hpi may attribute to bacterial shock as also seen in rock pool shrimp, *Palaemon elegans*, where its down-regulation is attributed to atrophy [31]. While this may be the case, DNAJ's gene expression stabilized later on at 6-hpi and 48-hpi, showing no significant difference from the control.

In summary, we may consider AHPND pathogenesis to be comprised of two aspects. These 2 aspects were clearly observable in the immune mechanisms affected by the VP_{AHPND} bacteria themselves, the partially purified toxin or both. RNA-seq determined a good number of candidate genes that were explored and validated by qPCR, giving good baseline information on the complex immune mechanism induced by what can be considered as two hallmarks of AHPND pathogenesis, bacterial shock and cellular stress by toxin. Three types of immune genes may thus be categorized during VP_{AHPND} infection: genes that are affected by the

VP_{AHPND} bacteria only, such as Serpin 3, clottable protein, and DNAJ homolog; genes that are affected by both VP_{AHPND} bacteria and partially purified toxin, such as crustin p, c-type lectin 3 and P38 MAPK; and genes that are affected by partially purified toxin only, such as *Lv*ALF. There is a possibility for *Lv*ALF's role in toxin neutralization of VP_{AHPND} in Pacific white shrimp highlighting and warranting further studies to characterize its wide range of binding ability.

Acknowledgements

The authors acknowledge the Marine Shrimp Broodstock Research Center II (MSBRC-2), Charoen Pokphand Foods PCL for providing *V. parahaemolyticus* AHPND. This research was supported by Thailand Research Fund (TRF Senior Scholar No. RTA5880004). The authors would also like to thank the support from Chulalongkorn University under the Ratchadaphisek Somphot Endowment to the Center of Excellence for Molecular Biology and Genomics of Shrimp and Outstanding Research Performance Program: Chulalongkorn Academic Advancement into Its 2nd Century Project (CUAASC). The Ratchadaphiseksomphot Endowment Fund for Postdoctoral Fellowship, Chulalongkorn University is also greatly appreciated.

Appendix A. Supplementary data

Supplementary data related to this article can be found at https://doi.org/10.1016/j.fsi.2018.06.054.

References

[1] E. Afgan, D. Baker, M. Van den beek, D. Blankenberg, D. Bouvier, M. Čech, J. Chilton, D. Clements, N. Coraor, C. Eberhard, B. Grüning, A. Guerler, J. Hillman-Jackson, G. Von kuster, E. Rasche, N. Soranzo, N. Turaga, J. Taylor, A. Nekrutenko, J. Goecks, The Galaxy platform for accessible, reproducible and collaborative biomedical analyses: 2016 update, Nucleic Acids Res. 44 (Web Server issue) (2016) W3–W10 http://doi.org/10.1093/nar/gkw343.

[2] S.F. Altschul, W. Gish, W. Miller, E.W. Myers, D.J. Lipman, Basic local alignment search tool, J. Mol. Biol. 215 (1990) 403–410.

[3] M. Ashburner, C.A. Ball, J.A. Blake, D. Botstein, H. Butler, J.M. Cherry, A.P. Davis, K. Dolinski, S.S. Dwight, J.T. Eppig, M.A. Harris, D.P. Hill, L. Issel-Tarver, A. Kasarskis, S. Lewis, J.C. Matese, J.E. Richardson, M. Ringwald, G.M. Rubin, G. Sherlock, Gene ontology: tool for the unification of biology. The Gene Ontology Consortium, Nat. Genet. 25 (2000) 25–29.

[4] D. Banerjee, B. Maiti, S. Girisha, M. Venugopal, I. Karunasagar, A crustin isoform from black tiger shrimp, *Penaeus monodon* exhibits broad spectrum anti-bacterial activity, Aquaculture Rep. 2 (2015) 106–111.

[5] H.M. Berman, J. Westbrook, Z. Feng, G. Gilliland, T.N. Bhat, H. Weissig, I.N. Shindyalov, P.E. Bourne, The protein data bank, 1999, International Tables for Crystallography Volume F: Crystallography of Biological Macromolecules (Pp. 675–684), Springer, Netherlands, 2006.

[6] P. Boonchuen, P. Jaree, A. Tassanakajon, K. Somboonwiwat, Hemocyanin of *Litopenaeus vannamei* agglutinates *Vibrio parahaemolyticus* AHPND (VP_{AHPND}) and neutralizes its toxin, Dev. Comp. Immunol. 84 (2018) 371–381 https://doi.org/10.1016/j.dci.2018.03.010.

[7] Y.-Y. Chen, J.-C. Chen, Y.-C. Lin, S.-T. Yeh, C.-L. Huang, White shrimp *Litopenaeus vannamei* that have received *Gracilaria tenuistipitata* extract show early recovery of immune parameters after ammonia stressing, Mar. Drugs 13 (2015).

[8] P. Cohen, The search for physiological substrates of MAP and SAP kinases in mammalian cells, Trends Cell Biol. 7 (1997) 353–361.

[9] S.R. Comeau, D.W. Gatchell, S. Vajda, C.J. Camacho, ClusPro: an automated docking and discrimination method for the prediction of protein complexes, Bioinformatics 20 (1) (2004) 45–50.

[10] A. Conesa, S. Gotz, J.M. Garcia-Gomez, J. Terol, M. Talon, M. Robles, Blast2GO: a universal tool for annotation, visualization and analysis in functional genomics research, Bioinformatics 21 (2005) 3674–3676.

[11] A. Cuenda, Mitogen-activated protein kinase kinase 4 (MKK4), Int. J. Biochem. Cell Biol. 32 (2000) 581–587.

[12] E. De La Vega, N.A. O'leary, J.E. Shockey, J. Robalino, C. Payne, C.L. Browdy, G.W. Warr, P.S. Gross, Anti-lipopolysaccharide factor in *Litopenaeus vannamei* (*Lv*ALF): a broad spectrum antimicrobial peptide essential for shrimp immunity against bacterial and fungal infection, Mol. Immunol. 45 (2008) 1916–1925.

[13] M.G. Grabherr, B.J. Haas, M. Yassour, J.Z. Levin, D.A. Thompson, I. Amit, X. Adiconis, L. Fan, R. Raychowdhury, Q. Zeng, Z. Chen, E. Mauceli, N. Hacohen, A. Gnirke, N. Rhind, F. Di Palma, B.W. Birren, C. Nusbaum, K. Lindblad-Toh, N. Friedman, A. Regev, Full-length transcriptome assembly from RNA-Seq data without a reference genome, Nat. Biotechnol. 29 (2011) 644–652.

[14] J.E. Han, K.F. Tang, L.H. Tran, D.V. Lightner, Photorhabdus insect-related (Pir) toxin-like genes in a plasmid of *Vibrio parahaemolyticus*, the causative agent of acute hepatopancreatic necrosis disease (AHPND) of shrimp, Dis. Aquat. Org. 113 (2015) 33–40.

[15] W. Humphrey, A. Dalke, K. Schulten, VMD: visual molecular dynamics, J. Mol. Graph. 14 (1) (1996) 33–38.

[16] M. Kanehisa, S. Goto, Y. Sato, M. Furumichi, M. Tanabe, KEGG for integration and interpretation of large-scale molecular data sets, Nucleic Acids Res. 40 (2012) D109–D114.

[17] M.R. Kanost, Serine proteinase inhibitors in arthropod immunity, Dev. Comp. Immunol. 23 (1999) 291–301.

[18] H. Kondo, S. Tinwongger, P. Proespraiwong, R. Mavichak, S. Unajak, R. Nozaki, I. Hirono, Draft genome sequences of six strains of *Vibrio parahaemolyticus* isolated from early mortality syndrome/acute hepatopancreatic necrosis disease shrimp in Thailand, Genome Announc. 2 (2014).

[19] D. Kozakov, D.R. Hall, B. Xia, K.A. Porter, D. Padhorny, C. Yueh, D. Beglov, S. Vajda, The ClusPro web server for protein-protein docking, Nat. Protoc. 12 (2) (2017) 255–278.

[20] H.-C. Lai, T.H. Ng, M. Ando, C.-T. Lee, I.T. Chen, J.-C. Chuang, R. Mavichak, S.-H. Chang, M.-D. Yeh, Y.-A. Chiang, H. Takeyama, H.-O. Hamaguchi, C.-F. Lo, T. Aoki, H.-C. Wang, Pathogenesis of acute hepatopancreatic necrosis disease (AHPND) in shrimp, Fish Shellfish Immunol. 47 (2015) 1006–1014.

[21] C. Lee, I. Chen, Y. Yang, T. Ko, Y. Huang, J. Huang, et al., The opportunistic marine pathogen *Vibrio parahaemolyticus* becomes virulent by acquiring a plasmid that expresses a deadly toxin, Proc. Natl. Acad. Sci. Unit. States Am. 112 (34) (2015) 10798–10803.

[22] J.-H. Leu, S.-H. Chen, Y.-B. Wang, Y.-C. Chen, S.-Y. Su, C.-Y. Lin, J.-M. Ho, C.-F. Lo, A review of the major penaeid shrimp EST studies and the construction of a shrimp transcriptome database based on the ESTs from four penaeid shrimp, Mar. Biotechnol. 13 (2011) 608–621.

[23] S. Li, S. Guo, F. Li, J. Xiang, Functional diversity of anti-lipopolysaccharide factor isoforms in shrimp and their characters related to antiviral activity, Mar. Drugs 13 (2015) 2602–2616.

[24] Y. Liu, F. Li, B. Wang, B. Dong, X. Zhang, J. Xiang, A serpin from Chinese shrimp *Fenneropenaeus chinensis* is responsive to bacteria and WSSV challenge, Fish Shellfish Immunol. 26 (2009) 345–351.

[25] Y. Liu, T. Liu, F. Hou, X. Wang, X. Liu, Lvserpin3 is involved in shrimp innate immunity via the inhibition of bacterial proteases and proteases involved in prophenoloxidase system, Fish Shellfish Immunol. 48 (2016) 128–135 https://doi.org/10.1016/j.fsi.2015.09.039.

[26] Y. Liu, Y. Sun, Q. Wang, F. Hou, X. Liu, Identification and functional characterizations of serpin8, a potential prophenoloxidase-activating protease inhibitor in Pacific white shrimp, *Litopenaeus vannamei*, Fish Shellfish Immunol. 60 (2017) 492–501 https://doi.org/10.1016/j.fsi.2016.11.024.

[27] Z. Luo, J. Zhang, F. Li, X. Zhang, C. Liu, J. Xiang, Identification of a novel C-type lectin from the shrimp *Litopenaeus vannamei* and its role in defense against pathogens infection, Chin. J. Oceanol. Limnol. 29 (2011) 942.

[28] M.B.B. Maningas, H. Kondo, I. Hirono, T. Saito-Taki, T. Aoki, Essential function of transglutaminase and clotting protein in shrimp immunity, Mol. Immunol. 45 (2008) 1269–1275.

[29] T. Methatham, P. Boonchuen, P. Jaree, A. Tassanakajon, K. Somboonwiwat, Antiviral action of the antimicrobial peptide ALF*Pm*3 from *Penaeus monodon* against white spot syndrome virus, Dev. Comp. Immunol. 69 (2017) 23–32.

[30] L. Nunan, D. Lightner, C. Pantoja, S. Gomez-Jimenez, Detection of acute hepatopancreatic necrosis disease (AHPND) in Mexico, Dis. Aquat. Org. 111 (2014) 81–86.

[31] P. Olsvik, B. Lunestad, A. Agnalt, O. Samuelsen, Impact of teflubenzuron on the rockpool shrimp (*Palaemon elegans*), Comp. Biochem. Physiol. C Toxicol. Pharmacol. 201 (2017) 35–43.

[32] M.W. Pfaffl, A new mathematical model for relative quantification in real-time RT-PCR, Nucleic Acids Res. 29 (2001) e45.

[33] K. Phiwsaiya, W. Charoensapsri, S. Taengphu, H. Dong, P. Sangsuriya, G. Nguyen, et al., A natural *Vibrio parahaemolyticus* Δ pirA Vp pirB Vp+ mutant kills shrimp but produces neither Pir Vp toxins nor acute hepatopancreatic necrosis disease lesions, Appl. Environ. Microbiol. 83 (16) (2017) e00680–17.

[34] S. Powell, D. Szklarczyk, K. Trachana, A. Roth, M. Kuhn, J. Muller, R. Arnold, T. Rattei, I. Letunic, T. Doerks, L.J. Jensen, C. Von Mering, P. Bork, eggNOG v3.0: orthologous groups covering 1133 organisms at 41 different taxonomic ranges, Nucleic Acids Res. 40 (2012) D284–D289.

[35] M. Punta, P.C. Coggill, R.Y. Eberhardt, J. Mistry, J. Tate, C. Boursnell, N. Pang, K. Forslund, G. Ceric, J. Clements, A. Heger, L. Holm, E.L.L. Sonnhammer, S.R. Eddy, A. Bateman, R.D. Finn, The Pfam protein families database, Nucleic Acids Res. 40 (2012) D290–D301.

[36] S. Pyronnet, Human eukaryotic translation initiation factor 4G (eIF4G) recruits Mnk1 to phosphorylate eIF4E, EMBO J. 18 (1) (1999) 270–279.

[37] Z. Qin, V. Babu, Q. Wan, M. Zhou, R. Liang, A. Muhammad, et al., Transcriptome analysis of Pacific white shrimp (*Litopenaeus vannamei*) challenged by *Vibrio parahaemolyticus* reveals unique immune-related genes, Fish Shellfish Immunol. 77 (2018) 164–174 https://doi.org/10.1016/j.fsi.2018.03.030.

[38] M.D. Robinson, D.J. Mccarthy, G.K. Smyth, edgeR: a Bioconductor package for differential expression analysis of digital gene expression data, Bioinformatics 26 (2010) 139–140.

[39] R. Rosa, A. Vergnes, J. de Lorgeril, P. Goncalves, L. Perazzolo, L. Sauné, B. Romestand, J. Fievet, Y. Gueguen, E. Bachère, D. Destoumieux-Garzón, Functional divergence in shrimp anti-lipopolysaccharide factors (ALFs): from recognition of cell wall components to antimicrobial activity, PLoS One 8 (7) (2013) e67937.

[40] R. Sirikharin, S. Taengchaiyaphum, P. Sanguanrut, T.D. Chi, R. Mavichak, P. Proespraiwong, B. Nuangsaeng, S. Thitamadee, T.W. Flegel, K. Sritunyalucksana,

Characterization and PCR detection of binary, Pir-like toxins from *Vibrio parahaemolyticus* isolates that cause acute hepatopancreatic necrosis disease (AHPND) in shrimp, PLoS One 10 (2015) e0126987.
[41] K. Somboonwiwat, M. Marcos, A. Tassanakajon, S. Klinbunga, A. Aumelas, B. Romestand, et al., Recombinant expression and anti-microbial activity of anti-lipopolysaccharide factor (ALF) from the black tiger shrimp, Dev. Comp. Immunol. 29 (10) (2005) 841–851.
[42] K. Somboonwiwat, E. Bachere, V. Rimphanitchayakit, A. Tassanakajon, Localization of anti-lipopolysaccharide factor (ALF*Pm*3) in tissues of the black tiger shrimp, *Penaeus monodon*, and characterization of its binding properties, Dev. Comp. Immunol. 32 (2008) 1170–1176.
[43] K. Somboonwiwat, V. Chaikeeratisak, H.C. Wang, C. Fang Lo, A. Tassanakajon, Proteomic analysis of differentially expressed proteins in *Penaeus monodon* hemocytes after *Vibrio harveyi* infection, Proteome Sci. 8 (2010) 39.
[44] S. Somnuk, A. Tassanakajon, V. Rimphanitchayakit, Gene expression and characterization of a serine proteinase inhibitor PmSERPIN8 from the black tiger shrimp *Penaeus monodon*, Fish Shellfish Immunol. 33 (2) (2012) 332–341.
[45] S.A. Soto-Rodriguez, B. Gomez-Gil, R. Lozano-Olvera, M. Betancourt-Lozano, M.S. Morales-Covarrubias, Field and experimental evidence of *Vibrio parahaemolyticus* as the causative agent of acute hepatopancreatic necrosis disease of cultured shrimp (*Litopenaeus vannamei*) in Northwestern Mexico, Appl. Environ. Microbiol. 81 (2015) 1689–1699.
[46] P. Supungul, S. Tang, C. Maneeruttanarungroj, V. Rimphanitchayakit, I. Hirono, T. Aoki, A. Tassanakajon, Cloning, expression and antimicrobial activity of crustin*Pm*1, a major isoform of crustin, from the black tiger shrimp *Penaeus monodon*, Dev. Comp. Immunol. 32 (2008) 61–70.
[47] A. Tassanakajon, K. Somboonwiwat, P. Supungul, S. Tang, Discovery of immune molecules and their crucial functions in shrimp immunity, Fish Shellfish Immunol. 34 (2013) 954–967.
[48] A. Tassanakajon, V. Rimphanitchayakit, S. Visetnan, P. Amparyup, K. Somboonwiwat, W. Charoensapsri, S. Tang, Shrimp humoral responses against pathogens: antimicrobial peptides and melanization, Dev. Comp. Immunol. 80 (2018) 81–93.
[49] L. Tran, L. Nunan, R.M. Redman, L.L. Mohney, C.R. Pantoja, K. Fitzsimmons, D.V. Lightner, Determination of the infectious nature of the agent of acute hepatopancreatic necrosis syndrome affecting penaeid shrimp, Dis. Aquat. Org. 105 (2013) 45–55.
[50] A. Untergasser, I. Cutcutache, T. Koressaar, J. Ye, B.C. Faircloth, M. Remm, S.G. Rozen, Primer3–new capabilities and interfaces, Nucleic Acids Res. 40 (2012) e115.
[51] X.-W. Wang, J.-X. Wang, Diversity and multiple functions of lectins in shrimp immunity, Dev. Comp. Immunol. 39 (2013) 27–38.
[52] X.-W. Wang, J.-D. Xu, X.-F. Zhao, G.R. Vasta, J.-X. Wang, A shrimp C-type lectin inhibits proliferation of the hemolymph microbiota by maintaining the expression of antimicrobial peptides, J. Biol. Chem. 289 (2014) 11779–11790.
[53] N. Wetsaphan, V. Rimphanitchayakit, A. Tassanakajon, K. Somboonwiwat, *Pm*SERPIN3 from black tiger shrimp *Penaeus monodon* is capable of controlling the proPO system, Dev. Comp. Immunol. 41 (2) (2013) 110–119.
[54] Y.T. Yang, I.T. Chen, C.T. Lee, C.Y. Chen, S.S. Lin, L.I. Hor, T.C. Tseng, Y.T. Huang, K. Sritunyalucksana, S. Thitamadee, H.C. Wang, C.F. Lo, Draft genome sequences of four strains of *Vibrio parahaemolyticus*, three of which cause early mortality syndrome/acute hepatopancreatic necrosis disease in shrimp in China and Thailand, Genome Announc. 2 (2014).
[55] M.-D. Yeh, H.-C. Wang, Characterization and involvement of Toll and IMD pathways in AHPND-infected shrimp, Fish Shellfish Immunol. 53 (2016) 62.
[56] M.D. Young, M.J. Wakefield, G.K. Smyth, A. Oshlack, Gene ontology analysis for RNA-Seq: accounting for selection bias, Genome Biol. 11 (2010) R14.
[57] F. Yue, L. Pan, P. Xie, D. Zheng, J. Li, Immune responses and expression of immune-related genes in swimming crab *Portunus trituberculatus* exposed to elevated ambient ammonia-N stress, Comp. Biochem. Physiol. Mol. Integr. Physiol. 157 (2010) 246–251.
[58] W. Zhan, X. Tang, X. Wang, L. He, X. Wei, An anti-lipopolysaccharide factor in *Litopenaeus vannamei* participates in the immune defense against WSSV and *Vibrio anguillarum*, J. Crustac Biol. 35 (5) (2015) 670–675.
[59] Y. Zhang, I-TASSER server for protein 3D structure prediction, BMC Bioinf. 9 (2008) 40.
[60] Y.R. Zhao, Y.H. Xu, H.S. Jiang, S. Xu, X.F. Zhao, J.X. Wang, Antibacterial activity of serine protease inhibitor 1 from kuruma shrimp *Marsupenaeus japonicus*, Dev. Comp. Immunol. 44 (2014) 261–269.